Reduced J_c Anisotropy and Enhanced In-Field Performance of Thick $BaHfO_3$-Doped $YBa_2Cu_3O_{7-\delta}$ Films on ABAD-YSZ Templates

Patrick Pahlke, Mayraluna Lao, Michael Eisterer, Alexander Meledin, Gustaaf Van Tendeloo, Jens Hänisch, Max Sieger, Alexander Usoskin, Jan Strömer, Bernhard Holzapfel, Ludwig Schultz, and Ruben Hühne

***Abstract*—Pure and 6 mol% $BaHfO_3$ (BHO)-doped $YBa_2Cu_3O_{7-\delta}$ (YBCO) films with a film thickness of around 1 μm were prepared on CeO_2-buffered ABAD-YSZ templates by pulsed laser deposition. The self-field J_c at 77 K reaches 1.1 MA/cm^2 in the doped sample compared with 2.5 MA/cm^2 in pure YBCO. Above a magnetic field of 2.2 T along $B \| c$, J_c of the BHO-doped sample exceeds the J_c of the undoped film. The maximum pinning force density ($F_{P,max}$) reaches a value of around 3 GN/cm^2 for both samples, but $B(F_{P,max})$ increases from 1.4 T (pure) to a value of 2.9 T (BHO:YBCO). The J_c anisotropy curves of the doped sample show a large and broad peak at $B \| c$ and a strongly reduced anisotropy at all temperatures and fields compared with the pure sample. A complex defect structure with $YBa_2Cu_4O_8$ intergrowths, Y_2O_3 precipitates, and BHO nanocolumns with a fan-shaped structure is observed by transmission electron microscopy investigations, which can explain the measured $J_c(B, \theta)$ behavior.**

***Index Terms*—$BaHfO_3$, coated conductors, nanocolumns, pinning, YBCO.**

I. Introduction

THE development of coated conductors with high current carrying capability for diverse applications is still a hot topic. Especially for the generation of high magnetic fields with superconducting coils it is essential to increase the critical current density in a wide angular range or to reduce the anisotropy. This can be realized by the incorporation of c-axis correlated secondary phases into the $YBa_2Cu_3O_{7-\delta}$ (YBCO) matrix such as $BaHfO_3$ (BHO). For our study, we use technical ABAD-YSZ templates which can be produced in long length [1] and focus on films with a thickness relevant for applications ($>$ 500 nm).

It was already shown that the incorporation of BHO can enhance the pinning force density and the irreversibility field in thick YBCO film prepared on technical Ni-9at%W (Ni9W) tape, where the highest values were achieved in the highest tested concentration of 6 mol% BHO [2]. We now transfer this knowledge to ABAD-YSZ templates.

The goal of this paper is a qualitative comparison of the $J_c(B, T, \theta)$ behavior in pure and 6 mol% BHO-doped YBCO films on ABAD-YSZ templates.

TABLE I
BASIC SAMPLE PROPERTIES

Property (Unit)	Pure YBCO	6 mol% BHO:YBCO
Thickness (nm)	1200	700
T_c (K)	90.2	88.2
c-axis (Å)	11.71	11.76

II. Experimentals

A. Sample Preparation

We used a 4 mm $\times$ 10 mm CeO_2-buffered ABAD-YSZ template, where the Y_2O_3-stabilized ZrO_2 (YSZ) was prepared by alternating beam assisted deposition (ABAD) on a stainless steel metal tape [1]. The sample was heated to 810 °C in a UHV chamber under an O_2 pressure of 0.4 mbar. Afterwards, the $YBa_2Cu_3O_{7-\delta}$ (YBCO) films were deposited by pulsed laser deposition (PLD) using a KrF excimer laser (COHERENT LPXpro 305, $\lambda = 248$ nm) at an energy density of 1.6 J/cm^2 at the target surface. We used a stoichiometric YBCO target and a target doped with 6 mol% (2.6 vol%) $BaHfO_3$ (BHO). Targets were mixed from single component powder in the desired stoichiometry, pressed and sintered. Even though we used the same laser conditions for the deposition of pure and BHO-doped films, we observed a different effective growth rate, leading to different film thicknesses (Table I). After oxygenation at 770 °C under 400 mbar O_2 partial pressure for 1 h, the sample was covered at room temperature with around 50 nm silver in another PLD system.

B. Structural Characterization

θ–2θ scans were performed with a Bruker D8 Advance Diffractometer (Co anode), and the c-axis lattice parameters

were calculated with the Nelson-Riley method [3]. Cross sections were prepared by focused ion-beam technique (FIB, FEI Helios Nanolab 600i), to determine the film thickness.

Transmission electron microscopy (TEM), bright-field transmission electron microscopy (BF TEM) and high-angle annular dark-field scanning transmission electron microscopy (HAADF-STEM) were performed on an FEI Titan electron microscope, equipped with an aberration corrector for the probe-forming lens as well as a high-brightness gun, operated at 300 kV and on an FEI Tecnai Osiris electron microscope operated at 200 kV. TEM cross sectional specimens were prepared via FEI Helios Nanolab 650 FIB. The samples were plasma cleaned before the TEM measurements.

C. Electrical Characterization

The transition temperature (T_c) was determined by an inductive method where the shielding of a magnetic field is monitored in dependence of temperature. The given inductively measured T_c value is comparable to the resistively determined $T_{c,10}$, where the 10% criterion of the extrapolated normal state resistance crosses the $R(T)$ curve. Maps of the critical current density (J_c) distribution in the sample were obtained by inversion of the trapped field profile measured by a scanning Hall probe device in liquid N_2 [4]. The listed values correspond to the self-field critical current density $J_{c,sf}$ at 77 K. The irreversibility field (B_{irr}) was determined by fitting $F_P(B) = J_c \times B$ with the empirical Dew-Hughes function [5]

$$F_P(B) \propto \left(\frac{B}{B_{irr}}\right)^p \left(1 - \frac{B}{B_{irr}}\right)^q \quad (1)$$

with parameters p and q, depending on pinning mechanism and microstructure. To reduce arbitrariness of the fit, the upper limit of q was set to 2.

The J_c anisotropy was obtained from magnetization loops measured using a vector vibrating sample magnetometer (VSM). The VSM is equipped with a split coil magnet that can apply fields up to 5 T, and the sample holder can be rotated with a precision of about 1°. The evaluation of J_c from the width of the hysteresis curve is valid only if the sample is at full field penetration. This leads us to the limitation of the method in evaluating J_c at $B \| ab$ as the penetrating field diverges.

III. Results and Discussion

A. Basic Structural and Electrical Properties

θ–2θ scans (Fig. 1) confirm a pure c-axis oriented growth of YBCO on the ABAD-YSZ template. The incorporation of BHO into the YBCO matrix leads to an elongated YBCO c-axis lattice parameter (Table I), which is in agreement with former studies on BHO [2] and $BaZrO_3$/$BaSnO_3$ doped films [6]. This is due to the biaxially aligned growth of BHO columns, which results in tensile strain of the c-axis to adapt the lattice parameters. The lattice parameter of the pseudocubic $BaHfO_3$ itself was determined from its 2θ position to be around 4.15 Å, which is close to the bulk value. Aside from the c-axis peaks, we observe a small Y_2O_3 (004) peak in the pure sample, which is not visible in the BHO doped sample. Most probably Y_2O_3 solutes in BHO, as already discussed in [2].

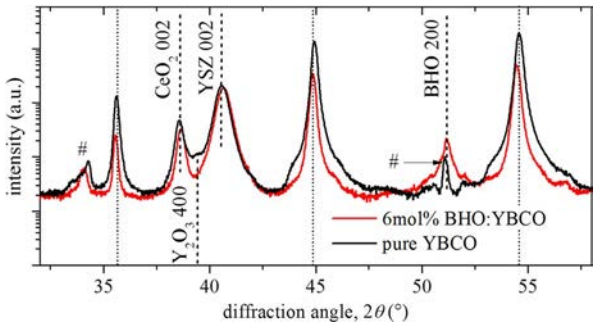

Fig. 1. θ–2θ-scans of the pure YBCO and the BHO:YBCO sample. Peaks of the metallic substrate are labeled with # and dotted lines indicate the position of the YBCO (00ℓ) peaks. The relatively broad BHO (200) peak is overlapped by a sharp substrate peak.

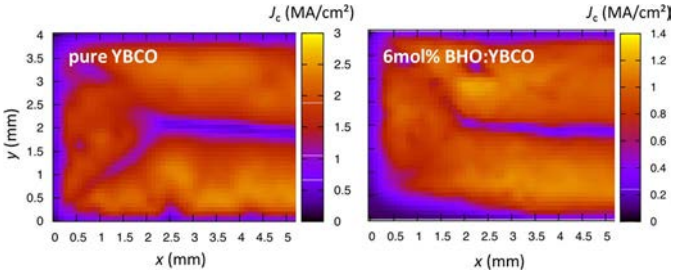

Fig. 2. J_c maps of one side of the pure and the BHO:YBCO sample with a spatial resolution of 100 μm were obtained from the inversion of the trapped field profiles. The values correspond to the self-field J_c at 77 K. The low J_c parts in the middle and the diagonals of the sample are an artifact of the inversion algorithm.

TABLE II
Electrical Properties at 77 K

Property (Unit)	Pure YBCO	6 mol %BHO:YBCO
$J_{c,sf}$ (MA/cm^2)	2.5±0.3	1.1±0.2
α-value	0.57	0.32
$F_{P,max}$ (GN/m^3)	3.2	3.0
$B(F_{P,max})$ (T)	1.4	2.9
p	0.55	0.85
q	2.0	1.5
B_{irr} (T)	6.6	8.0

The T_c of the BHO-doped sample is around 2 K lower than of the pure YBCO sample (Table I), which was also reported for similar films on Ni9W-tape [2]. The transition widths are in both cases below 1 K, indicating good sample homogeneity.

Using the J_c maps (Fig. 2), we can determine a typical $J_{c,sf}$ value of 2.5 MA/cm^2 for the pure YBCO film and a value of 1.1 MA/cm^2 for the BHO doped sample (Table II), i.e., $J_{c,sf}$ is strongly influenced by the doping. In contrast, in BHO-doped YBCO on NiW tape, $J_{c,sf}$ is independent of the BHO content [2], due to the more dominant grain boundary limitation at low fields.

B. Field Dependence of J_c at 77 K

Whereas the undoped sample shows higher J_c values at low magnetic fields, the BHO-doped sample outperforms the pure YBCO sample above a crossing point at around 2.2 T (Fig. 3). The $J_c(B)$ curves can be fitted by the relation $J_c(B) \sim B^{-\alpha}$ in the field range between 0.04 T and 0.8 T, where the power law

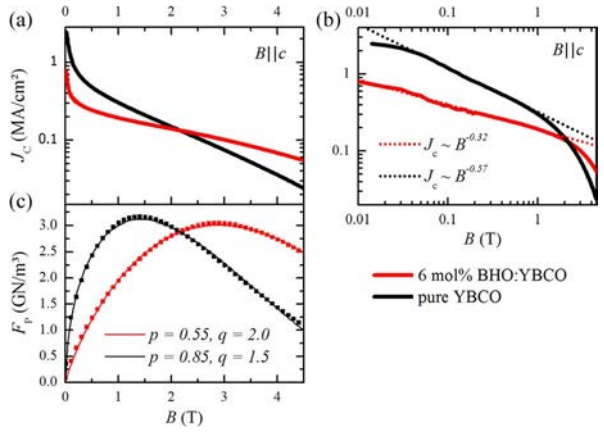

Fig. 3. Field dependence of J_c at 77 K in (a) single logarithmic and (b) double logarithmic scale and (c) of pinning force density F_P of the pure and the BHO:YBCO sample. In (c), the fitting according to relation (1) is shown using the parameters listed in Table II, and only every tenth data point is plotted.

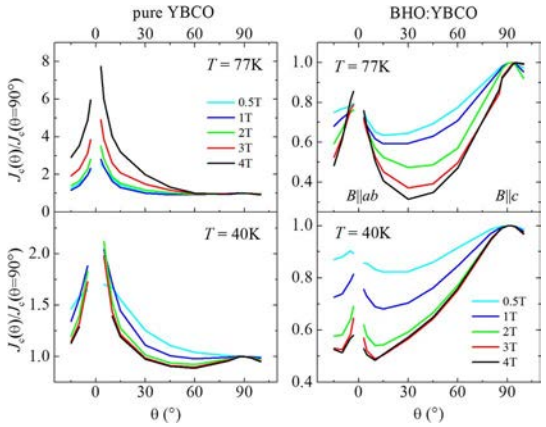

Fig. 4. Angular dependence of J_c normalized to the value at $\Theta = 90°$ $(B||c)$ for two different temperatures and applied fields of 0.5 to 4 T. Note that the scaling is different.

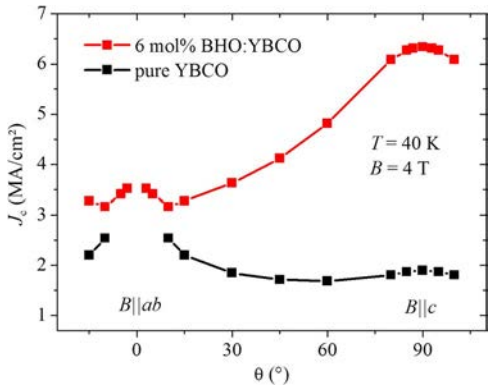

Fig. 5. $J_c(\theta)$-curve for the pure and the BHO:YBCO sample at a magnetic field of 4 T and a temperature of 40 K.

exponent α is 0.57 in the pure and 0.32 in the BHO-doped sample. These values agree quite well with earlier measurements on undoped ($\alpha \sim 0.5 - 0.6$ [7], [8]) and doped samples ($\alpha \sim 0.33$ [9]). The crossing point of both J_c curves generally depends on the $J_{c,sf}$ value and the slope α of the curves. Especially $J_{c,sf}$ is also depending on the film thickness. In 700 nm thick pure YBCO samples an even higher $J_{c,sf}$ of around 2.7 MA/cm^2 is expected at 77 K [10], meaning the crossing point would shift to slightly higher fields. But as the pinning mechanism is not expected to change in this thickness range, it is reasonable to compare these samples qualitatively.

The maximal value of the pinning force density is quite similar for both samples (∼3.1 GN/m^3, Table II), but the field $B_{max} = B(F_{P,max})$ at which the maximal pinning force is achieved is much larger in the BHO-doped sample ($B_{max} = 2.9$ T) than in the pure one ($B_{max} = 1.4$ T). Furthermore, the F_P peak of the BHO sample is much broader, pointing to effective pinning centers in a wider field range.

The best agreement of fitting the $F_P(B)$-data by relation (1) was found when q was set to 2 for the undoped sample and 1.5 for the doped sample [see fitting in Fig. 3(c)]. The p-value of the doped sample is larger than in the undoped one. This correlates to a smaller α-value in the low B-region, where the first term in relation (1) dominates and $p = 1 - \alpha$. Additionally, B_{irr} is increased to 8 T by doping.

C. Angular Dependence of J_c

Anisotropy measurements were carried out at 77 K and 40 K in the field range from 0.5 T to 4 T. For a better visualization, the $J_c(\theta)$ curves at different B were normalized to their values at $\theta = 90°$ $(B||c)$ (Fig. 4).

The pure sample exhibits a large peak at $\theta = 0°$ $(B||ab)$ and a smaller peak at $\theta = 90°$ $(B||c)$ which becomes more visible at lower temperature in high magnetic fields. The anisotropy value $A = J_c(\theta)_{max}/J_c(\theta)_{min}$ reaches ∼8 at 77 K and ∼2.5 at 40 K for a magnetic field of 4 T. In contrast, the anisotropy value in the doped sample is lower $(A \sim 2)$ and nearly independent of temperature. In general, we observe an increased anisotropy with increasing field in both samples. In the doped sample, we also find an ab-peak, but additionally a broad and more dominant c-axis peak, pointing to very effective pinning centers parallel to the c-axis. Particularly at 77 K, the pinning in c-direction is as strong as in ab-direction and almost independent of the magnetic field, but at 40 K it becomes much stronger with increasing field. Already at $B = 4$ T and $T = 40$ K, J_c of the doped sample is higher compared to the undoped sample at all field angles (Fig. 5).

D. Microstructure

TEM images of the undoped sample show a dense film with a weak light-dark contrast parallel to YBCO c-axis direction over the whole film thickness. We attribute this to slightly misoriented YBCO columns (mainly rotation around c-axis), which are caused by the ABAD-YSZ crystallites through the CeO_2 cap layer [11]. These small angle [001]-tilt boundaries, are assumed to be mainly responsible for the small peak in the angular dependence at $\theta = 90°$ $(B||c)$ in the undoped film (Fig. 4).

TEM images of the BHO-doped sample show a flat and dense film with a complex microstructure, featuring a few nanoscaled Y_2O_3 precipitates with a size of around 10 nm, $YBa_2Cu_4O_8$ (Y124) intergrowths and BHO nanocolumns with a typical diameter of 3 nm to 5 nm (Fig. 6). The nucleation of the BHO columns starts right on the CeO_2 buffer layer, and some

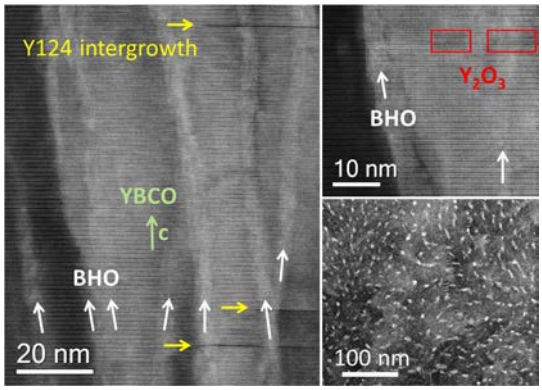

Fig. 6. HAADF STEM Z-contrast image showing nanoscale Y_2O_3 precipitates, $YBa_2Cu_4O_8$ (Y124) intergrowth, and tilted BHO nanocolumns with a typical diameter of 3 to 5 nm.

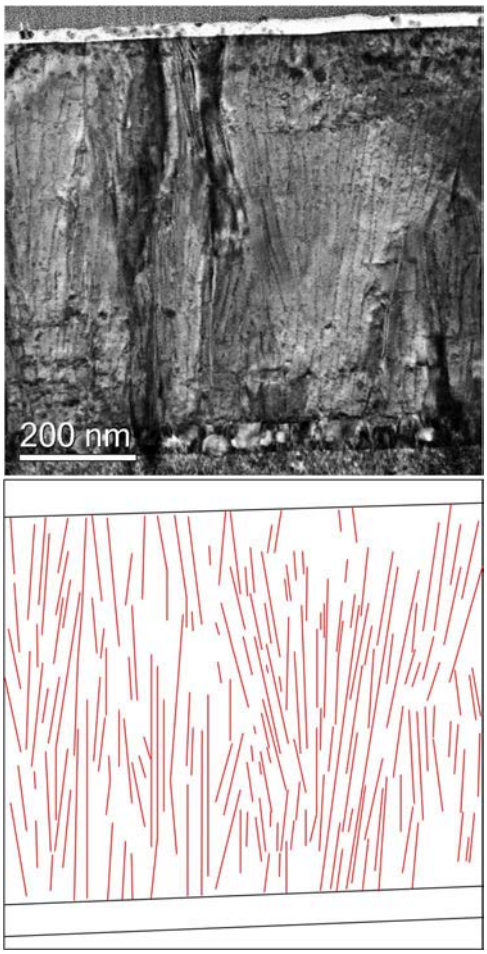

Fig. 7. (Upper part) BF TEM image of the cross section of the BHO-doped sample. (Lower part) Drawing of the length and orientation of clearly identifiable BHO nanocolumns showing a fan-shaped structure.

columns can be tracked almost the whole thickness of the film. We find two kinds of areas. In some parts, the columns grow straighter and parallel to the YBCO c-axis and so to the film normal direction. In other regions, we observe a fan-shaped growth of BHO (Fig. 7). High-resolution images of fan-shaped areas (Fig. 6) show that these columns are tilted and winding, still being biaxial oriented to YBCO. The tilt angle of the BHO columns towards the YBCO c-axis is about 10° for long pieces (length ∼400 nm) and up to 20° for shorter segments (length ∼100 nm). This could explain why the c-axis peak in the J_c anisotropy curve is broad and the addition of BHO leads to an increased J_c in a wide angular range.

A similar structural formation of tilted columns of dopant material has been observed in YBCO films with YSZ and $BaZrO_3$ doping [6], [9], and in BHO doped $SmBa_2Cu_3O_y$ films [12], [13] prepared by PLD on single crystalline substrates. In all these cases an enhanced performance of J_c (B) at $B\|c$ was measured and in [6] and [9] a broad and dominant peak was observed in the angular measurement at $B\|c$.

IV. Conclusion

6 mol% BHO doping was successfully implemented into YBCO based coated conductors prepared on ABAD-YSZ templates. We find a fan-shaped growth of BHO nanocolumns which lead to a broad peak in the anisotropy curves around $B\|c$ and a reduction of the J_c anisotropy. The effect of these pinning centers is more dominant at higher fields and lower temperature. In comparison to the undoped reference sample the BHO sample shows a better J_c performance at all field angles at 40 K and 4 T.

Acknowledgment

The authors gratefully acknowledge J. Scheiter, U. Fiedler, and M. Kühnel for technical assistance.

References

[1] A. Usoskin *et al.*, "Processing of long-length YBCO coated conductors based on stainless steel tapes," *IEEE Trans. Appl. Supercond.*, vol. 17, no. 2, pp. 3235–3238, Jun. 2007.

[2] M. Sieger *et al.*, "$BaHfO_3$-doped thick $YBa_2Cu_3O_{7-\delta}$ films on highly alloyed textured Ni-W tapes," *IEEE Trans. Appl. Supercond.*, vol. 25, no. 3, Jun. 2015, Art. no. 6602604.

[3] J. B. Nelson and D. P. Riley, "An experimental investigation of extrapolation methods in the derivation of accurate unit-cell dimensions of crystals," in *Proc. Phys. Soc.*, vol. 57, no. 3, pp. 160–177, May 1945.

[4] F. Hengstberger, M. Eisterer, M. Zehetmayer, and H. W. Weber, "Assessing the spatial and field dependence of the critical current density in YBCO bulk superconductors by scanning Hall probes," *Supercond. Sci. Technol.*, vol. 22, no. 2, Jan. 2009, Art. no. 025011.

[5] D. Dew-Hughes, "Flux pinning mechanisms in type II superconductors," *Philosoph. Mag.*, vol. 30, no. 2, pp. 293–305, Aug. 1974.

[6] P. Mele *et al.*, "Ultra-high flux pinning properties of $BaMO_3$-doped $YBa_2Cu_3O_{7-x}$ thin films $(M = Zr, Sn)$," *Supercond. Sci. Technol.*, vol. 21, no. 3, Feb. 2008, Art. no. 032002.

[7] F. C. Klaassen *et al.*, "Vortex pinning by natural linear defects in thin films of $YBa_2Cu_3O_{7-\delta}$," *Phys. Rev. B*, vol. 64, 2001, Art. no. 184523.

[8] B. Dam *et al.*, "Origin of high critical currents in $YBa_2Cu_3O_{7-\delta}$ superconducting thin films," *Nature*, vol. 399, pp. 439–442, Jun. 1999.

[9] P. Mele *et al.*, "Enhanced high-field performance in PLD films fabricated by ablation of YSZ-added $YBa_2Cu_3O_{7-x}$ target," *Supercond. Sci. Technol.*, vol. 20, no. 3, pp. 244–250, Jan. 2007.

[10] P. Pahlke *et al.*, "Thick high J_c YBCO films on ABAD-YSZ templates," *IEEE Trans. Appl. Supercond.*, vol. 25, no. 3, Jun. 2015, Art. no. 6603804.

[11] P. Pahlke *et al.*, "Local orientation variations in YBCO films on technical substrates—A combined SEM and EBSD study," *IEEE Trans. Appl. Supercond.*, to be published. [Online]. Available: 10.1109/TASC.2016.2535138.

[12] S. Miura *et al.*, "Characteristics of high-performance $BaHfO_3$ doped $SmBa_2Cu_3O_y$ superconducting films fabricated with a seed layer and low-temperature growth," *Supercond. Sci. Technol.*, vol. 28, no. 6, pp. 65 013–65 020, Jun. 2015.

[13] S. Miura *et al.*, "Improvement in J_c performance below liquid nitrogen temperature for $SmBa_2Cu_3O_y$ superconducting films with $BaHfO_3$ nanorods controlled by low-temperature growth," *APL Mater.*, vol. 4, no. 1, Jan. 2016, Art. no. 016102.

Karlsruher Institut für Technologie

OPEN ACCESS

Repository KITopen

Dies ist ein Postprint/begutachtetes Manuskript.

Empfohlene Zitierung:

Pahlke, P.; Lao, M.; Eisterer, M.; Meledin, A.; Van Tendeloo, G.; Hänisch, J.; Sieger, M.; Usoskin, A.; Stromer, J.; Holzapfel, B.; Schultz, L.; Huhne, R.
Reduced Jc Anisotropy and Enhanced In-Field Performance of Thick $BaHfO_3$-Doped YBa_2Cu_3O7-δ Films on ABAD-YSZ Templates.
2016. IEEE transactions on applied superconductivity
doi: 10.5445/IR/1000055366

Zitierung der Originalveröffentlichung:

Pahlke, P.; Lao, M.; Eisterer, M.; Meledin, A.; Van Tendeloo, G.; Hänisch, J.; Sieger, M.; Usoskin, A.; Stromer, J.; Holzapfel, B.; Schultz, L.; Huhne, R.
Reduced Jc Anisotropy and Enhanced In-Field Performance of Thick $BaHfO_3$-Doped YBa_2Cu_3O7-δ Films on ABAD-YSZ Templates.
2016. IEEE transactions on applied superconductivity, 26 (3), 6603104.
doi:10.1109/TASC.2016.2541998

Lizenzinformationen: KITopen-Lizenz